Supplementary Material

Details of Model Implementation

The source code for this paper can be found online at: https://github.com/brianhhu/Contour_BOS. One pixel in our model input represents the typical size of the receptive field for a V1 edge cell (which at eccentricity 5 deg is about 0.7 deg, Chen *et al.* 2014). The simulated visual field is assumed to be homogeneous (*i.e.*, we neglect the influence of the cortical magnification factor). Each neuronal unit in the model represents multiple neurons with overlapping receptive fields and similar tuning. It is referred to as a "neuron" in the following and it is represented by an ordinary differential equation, eq. 1. For all examples the system is simulated for 0.5s and an equilibrium is reached within a few tens or about hundred simulated ms. A typical simulation of a visual field of 64×64 units consists of 30,528 coupled ordinary differential equations which are solved using a fourth-order Runge-Kutta algorithm in MATLAB.

Each neuron is characterized by its spatial location, its type (edge cell, object grouping cell, *etc.*) and one additional property, as follows. E cells are indexed by the angle of their preferred orientation: 0, $\pi/4$, $\pi/2$, and $3\pi/4$ (all angles relative to the horizontal). B cells are indexed by the angle of their preferred side of figure: right, 0; upper right, $\pi/4$; up, $\pi/2$; upper left, $3\pi/4$; left, π; lower left, $5\pi/4$; down, $3\pi/2$; lower right, $7\pi/4$. Note that the preferred side of a B cell is always orthogonal to its preferred orientation. Contour grouping cells are indexed by their preferred orientation (0, $\pi/4$, $\pi/2$, and $3\pi/4$), while object grouping neurons are selective for annuli of a preferred radius. As discussed earlier, we only use one preferred radius in this model, which we chose as corresponding to 16 pixels in the input layer. The network receives two types of inputs. A binary edge map activates E cells, taking value 1 if an edge of that orientation is present at this location in the image and (-1) otherwise. Finally, an attentional field stimulates grouping cells, with maximal strength of 0.07. This value is listed in Table 1, as are those of all other model parameters.

In the following, we define the anatomical connection patterns between all neuronal populations in our model. Obviously, this defines the receptive (and projective) fields of all model neurons. At the input level, edge cells (E population) receive one-to-one connections from input units (IN population) of the respective preferred orientations o_i at position (x, y), resulting in a connectivity weight distribution as follows,

$$WIN^{o_1}_{x,y} E^{o_2}_{x,y} = \begin{cases} intoe_w & if\ o_1 = o_2 \\ -1 & otherwise \end{cases} \tag{S1}$$

where the weight of the input to edge cell connections, $intoe_w$ is a scaling parameter, and its value is set to 1. Changing it does not produce different activation patterns in the network but rather scales up all activities. This is indicated in Table 1 by an asterisk (*) next to the value of this parameter, as well as to that of all others with this property.

The connections from edge cells to inhibitory IE cells are two-dimensional isotropic Gaussians:

$$WE_{x_1,y_1} IE_{x_2,y_2} = N_{etoie}\ \exp\left(-\frac{(x_1 - x_2)^2}{2\, etoie^2_{sd}} - \frac{(y_1 - y_2)^2}{2\, etoie^2_{sd}}\right) \tag{S2}$$

where the normalization coefficient N_{etoie} is determined from:

$$etoie_w = \sum_{i,j=-24}^{24} WE_{x,y} IE_{x+i,y+j} \tag{S3}$$

The weight of the edge to IE connections $etoie_w$ is set to 8. The standard deviation of the lateral connections, $etoie_{sd}$ was chosen to be eight times the size of the edge cells' receptive field size. For simplicity, all lateral connections in V1 are assumed to have the same standard deviation. The upper limit in the sum of eq. S3 is where we truncate the Gaussian distribution used to define the connectivities, at three times its standard deviation (8), equal to 24 times the size of a V1 RF.

IE cells are not orientation selective, and inhibit all edge cells in their neighborhood. The strength of inhibition is independent of the preferred orientation of the edge cells and has the same pattern as the reciprocal edge to IE cell connections:

$$WIE_{x_1,y_1} E_{x_2,y_2} = N_{ietoe}\ \exp\left(-\frac{(x_1 - x_2)^2}{2\, ietoe^2_{sd}} - \frac{(y_1 - y_2)^2}{2\, ietoe^2_{sd}}\right) \tag{S4}$$

where the normalization coefficient N_{ietoe} is determined from:

$$ietoe_w = \sum_{i,j=-24}^{24} WIE_{x,y} E_{x+i,y+j} \tag{S5}$$

The strength of the inhibitory connections IE to edge cells, $ietoe_w$, is an important parameter in the model. Its value was chosen to be -8, which is just strong enough for the inhibition of the edge cells to cancel out activity in the case of a uniform stimulation field. In our model, attention in the absence of edges is a broad field, and experimental observations show little effect of attention alone on the firing rates of purely sensory (edge) cells. E cells locally connect to other edge cells of the same preferred orientation. These

connections allow for the passing of contour information along a line. The connection weights are,

$$
\begin{aligned}
WE^{o_1}_{x_1,y_1} E^{o_2}_{x_2,y_2} &= N_{etoe}\ \delta_{o_1,o_2}\ \delta_{y_1,0}\ \delta_{y_2,0}\ \exp\left(-\frac{(x_1-x_2)^2}{2\,etoe_{sd}^2}\right) \text{ if } o_1, o_2 = 0 \\
WE^{o_1}_{x_1,y_1} E^{o_2}_{x_2,y_2} &= N_{etoe}\ \delta_{o_1,o_2}\ \delta_{x_1,y_1}\ \delta_{x_2,y_2}\ \exp\left(-\frac{(x_1-x_2)^2}{2\,etoe_{sd}^2}\right) \text{ if } o_1, o_2 = \pi/4 \\
WE^{o_1}_{x_1,y_1} E^{o_2}_{x_2,y_2} &= N_{etoe}\ \delta_{o_1,o_2}\ \delta_{x_1,0}\ \delta_{x_2,0}\ \exp\left(-\frac{(y_1-y_2)^2}{2\,etoe_{sd}^2}\right) \text{ if } o_1, o_2 = \pi/2 \\
WE^{o_1}_{x_1,y_1} E^{o_2}_{x_2,y_2} &= N_{etoe}\ \delta_{o_1,o_2}\ \delta_{x_1,-y_1}\ \delta_{x_2,-y_2}\ \exp\left(-\frac{(y_1-y_2)^2}{2\,etoe_{sd}^2}\right) \text{ if } o_1, o_2 = 3\pi/4
\end{aligned}
\tag{S6}
$$

where the normalization coefficient N_{etoe} is determined from:

$$
etoe_w = \sum_{i,j=-24}^{24} WE^{o}_{x,y} E^{o}_{x+i,y+j} \tag{S7}
$$

The weight of the excitatory lateral connections $etoe_w = 2/3$ is chosen such that individual excitatory connections are stronger than the nonspecific inhibitory connections for a line of cells along the preferred direction, and that the integral of the excitatory connections is smaller than the integral of the inhibitory ones. The standard deviation $etoe_{sd} = 8$ is the same as for all other lateral connections in V1.

The edge cells E excite a pair of border-ownership cells with the same preferred orientation o_1 and at the same position, (x_i, y_i). Border ownership selective cells have opposite side-of-figure preferences o_2 which are orthogonal to o_1 (*i.e.* differing by $\pi/2$ in either direction). They are generated by connections from E cells whose weight is given by a 2D Gaussian,

$$
\begin{aligned}
WE^{o_1}_{x_1,y_1} B^{o_2}_{x_2,y_2} &= etob_w\ \exp\left(-\frac{(x_1-x_2)^2}{2\,etob_{sd}^2} - \frac{(y_1-y_2)^2}{2\,etob_{sd}^2}\right) \\
&o_1 \in \{0, \pi/4, \pi/2, 3\pi/4\} \\
&o_2 \in \{0, \pi/4, \pi/2, 3\pi/4, \pi, 5\pi/4, 3\pi/2, 7\pi/4\ \}
\end{aligned}
\tag{S8}
$$

where the weight of the E to border-ownership connections, $etob_w$ is set to 1.

The connections from border-ownership to inhibitory IB cells are two-dimensional Gaussians:

$$
WB_{x_1,y_1} IB_{x_2,y_2} = N_{btoib}\ \exp\left(-\frac{(x_1-x_2)^2}{2\,btoib_{sd}^2} - \frac{(y_1-y_2)^2}{2\,btoib_{sd}^2}\right) \tag{S9}
$$

where the normalization coefficient N_{btoib} is determined from:

$$
btoib_w = \sum_{i,j=-12}^{12} WB_{x,y} IB_{x+i,y+j} \tag{S10}
$$

The weight of the border-ownership to IB connections $btoib_w$ is set to 2. The standard deviation of the lateral connections, $btoib_{sd}$ was chosen to be four times the size of the border-ownership cells' receptive field size. For simplicity, all lateral connections in V2 are assumed to have the same standard deviation.

IB cells, which are not orientation selective, inhibit all border-ownership in their neighborhood with the same pattern as B to IB cell excitation:

$$
WIB_{x_1,y_1} B_{x_2,y_2} = N_{ibtob}\ \exp\left(-\frac{(x_1-x_2)^2}{2\,ibtob_{sd}^2} - \frac{(y_1-y_2)^2}{2\,ibtob_{sd}^2}\right) \tag{S11}
$$

where the normalization coefficients N_{ibtob} is determined from:

$$
ibtob_w = \sum_{i,j=-12}^{12} WIB_{x,y} B_{x+i,y+j} \tag{S12}
$$

The strength of the inhibitory connections IB to border-ownership, $ibtob_w$, is an important parameter in the model. Its value was chosen to be -2, which is just strong enough for the inhibition of the border-ownership cells to cancel out activity in the case of a uniform stimulation field. In our model, attention in the absence of edges is a broad field, and experimental observations show little effect of attention alone on the firing rates of border-ownership cells. This parameter also influences the value of the attention modulation of the non-preferred border ownership cells, and the value which was a priori chosen reproduces well the observed experimental value.

B cells connect to other border-ownership cells of the same preferred side of figure. These connections allow the passing of border ownership signal along a line:

$$WB^{o1}_{x_1,y_1}B^{o2}_{x_2,y_2} = N_{btob}\,\delta_{o_1,o_2}\,\delta_{x_1,0}\,\delta_{x_1,0}\,\exp\left(-\frac{(y_1-y_2)^2}{2\,btob^2_{sd}}\right)\quad o_1,o_2\in\{0,\pi\}$$

$$WB^{o1}_{x_1,y_1}B^{o2}_{y_2,y_2} = N_{btob}\,\delta_{o_1,o_2}\,\delta_{x_1,-y_1}\,\delta_{x_2,-y_2}\,\exp\left(-\frac{(y_1-y_2)^2}{2\,etoe^2_{sd}}\right)\quad o_1,o_2\in\{\pi/4,5\pi/4\}$$

$$WB^{o1}_{x_1,y_1}B^{o2}_{x_2,y_2} = N_{btob}\,\delta_{o_1,o_2}\,\delta_{y_1,0}\,\delta_{y_2,0}\,\exp\left(-\frac{(x_1-x_2)^2}{2\,btob^2_{sd}}\right)\quad o_1,o_2\in\{\pi/2,3\pi/2\}$$

$$WB^{o1}_{x_1,y_1}B^{o2}_{x_2,y_2} = N_{btob}\,\delta_{o_1,o_2}\,\delta_{x_1,y_1}\,\delta_{x_2,y_2}\,\exp\left(-\frac{(x_1-x_2)^2}{2\,btob^2_{sd}}\right)\quad o_1,o_2\in\{3\pi/4,7\pi/4\} \tag{S13}$$

where the normalization coefficient N_{btob} is determined from:

$$btob_w = \sum_{i,j=-12}^{12} WB^o_{x,y}B^o_{x+i,y+j} \tag{S14}$$

The weight of the excitatory lateral connections $btob_w = 2/3$ is chosen such that individual excitatory connections are stronger than the nonspecific inhibitory connections for a line of cells along the preferred direction, and that the integral of the excitatory connections is smaller than the integral of the inhibitory ones. The standard deviation $btob_{sd} = 4$ is the same as for all other lateral connections in V2.

B cells also connect to other border-ownership cells of orthogonal preferred orientation. These connections allow the passing of border ownership information along a corner, where rot is a rotation operator that rotates the connection matrix C_f by the angle o:

$$\begin{aligned} WB^{o1}_{x_1,y_1}B^{o2}_{x_2,y_2} = {} & btob_{wc}\,(\mathrm{rot}_{o_1}(C_f(x_2-x_1,y_2-y_1))\delta_{o_1,o_2-\pi/2} \\ & + c\,\mathrm{rot}_{o_1+\pi}(C_f(x_2-x_1,y_2-y_1))\delta_{o_1,o_2-\pi/2} \\ & + \mathrm{rot}_{o_2}(C_b(x_2-x_1,y_2-y_1))\delta_{o_1,o_2+\pi/2} \\ & + c\,\mathrm{rot}_{o_2+\pi}(C_b(x_2-x_1,y_2-y_1))\delta_{o_1,o_2+\pi/2}) \end{aligned} \tag{S15}$$

with the matrices

$$C_f(x,y) = \begin{cases} N_{btobc}\,\exp(-\frac{x^2+y^2}{2\,btob^2_{sd}}) & if\ x\geq 0\ \&\ y<0 \\ 0 & otherwise \end{cases} \tag{S16}$$

$$C_b(x,y) = \begin{cases} N_{btobc}\,\exp(-\frac{x^2+y^2}{2\,btob^2_{sd}}) & if\ x\geq 0\ \&\ y>0 \\ 0 & otherwise \end{cases} \tag{S17}$$

and the normalization coefficient N_{btobc} is obtained from

$$1 = \sum_{i,j=-12}^{12} C_f(i,j) \tag{S18}$$

The values of $btob_{wc} = 2/3$ and $c = 2/3$ were chosen to be the same as $btob_w$.

The connections from border-ownership cells to object grouping cells consist of 2D Gaussians rotated to the appropriate angle and arranged in a circular fashion, where $btogo_{sds}$ and $btog_{sdl}$ are the spreads of the Gaussian in the radial and tangential directions, respectively:

$$\begin{aligned} WB^o_{x_1,y_1}G^r_{x_2,y_2} = {} & \mathrm{rot}_o\left(N_{btogr}\,\exp\left(-\frac{(x_1-x_2+r)^2}{2\,(btogo_{sds}r)^2}-\frac{(y_1-y_2)^2}{2\,(btog_{sdl}r)^2}\right)\right) \\ & o\in\{0,\pi/4,\pi/2,3\pi/4,\pi,5\pi/4,3\pi/2,7\pi/4\} \end{aligned} \tag{S19}$$

where the normalization coefficient N_{btogr} is

$$btog_w = \sum_{i=-2r}^{2r} WB^0_{x-r,y+i}G^r_{x,y} \tag{S20}$$

The strength of the border-ownership to grouping connections $btog_w$, is a scaling parameter and was chosen to be 0.125, since in the model there are 4 preferred orientations and two side-of-figure preferences (8 total orientations) for the border-ownership cells, each of which sends input to each grouping cell. Each orientation of border-ownership cells provides a 2D Gaussian input to the grouping cells, with the standard deviation on the direction orthogonal to the radius being 0.5 times the radius, while the standard deviation on the direction parallel to the radius is 0.25 times the radius. (If these standard deviations are too large, then grouping cells lose specificity and, for more complicated images, some edges are assigned incorrectly. If these standard deviations are too small,

the density of grouping cells needs to be increased.) The distance between two neighboring cells of radius r is $r/2$, such that a line is never more than one standard deviation away from the center of a patch of connections involved in its grouping.

The feedback from the object grouping cells to lower level feature-selective neurons follows a similar spatial pattern of the B to object grouping connections. The feedback to E and B are similar, except E cells receive feedback with twice the radius and standard deviations to account for upsampling to twice the number of neurons in the V1 layer:

$$\begin{aligned} WG^{r}_{x_2,y_2}B^{o_1}_{x_1,y_1} &= \mathrm{rot}_{o_1}\left(N_{gtobr}\ \exp\left(-\frac{(x_1-x_2+r)^2}{2\,(btogo_{sds}r)^2}-\frac{(y_1-y_2)^2}{2\,(btog_{sdl}r)^2}\right)\right)\\ WG^{r}_{x_2,y_2}E^{o_2}_{x_1,y_1} &= \mathrm{rot}_{o_2+\pi/2}\left(N_{gtoer}\ \exp\left(-\frac{(x_1-x_2+(2r))^2}{2\,(btogo_{sds}(2r))^2}-\frac{(y_1-y_2)^2}{2\,(btog_{sdl}(2r))^2}\right)\right)\\ &\quad+\mathrm{rot}_{o_2+3\pi/2}\left(N_{gtoer}\ \exp\left(-\frac{(x_1-x_2+(2r))^2}{2\,(btogo_{sds}(2r))^2}-\frac{(y_1-y_2)^2}{2\,(btog_{sdl}(2r))^2}\right)\right)\\ o_1 &\in \{0,\pi/4,\pi/2,3\pi/4,\pi,5\pi/4,3\pi/2,7\pi/4\ \}\\ o_2 &\in \{0,\pi/4,\pi/2,3\pi/4\} \end{aligned} \tag{S21}$$

Since the number of the grouping cells on a line is inverse proportional to their scale, the line integral of the weight is considered proportional to the radius of the G cell:

$$gtob_w = \sum_{i=-2r}^{2r} WG^{r}_{x,y}B^{\pi}_{x+r,y+i} \tag{S22}$$

The value of $gtob_w = 2/3$ is critical for the model, and the border ownership modulation index depends critically on it. In order to reproduce the observed attention modulation of the nonpreferred side of figure for B cells, the weight of the feedback to edge cells needs to be four times that to the border ownership cells $gtoe_w = 8/3$.

In previous work (Mihalas et al, 2011), in order to fit the observed reaction time cost observed when irelevant objects are outside the focus of attention, a feedback from G to IG cells is introduced. Here, this connection allows for competition between different grouping neurons. This has the same pattern, but half the scaled weight as the feedback to B cells and twice its standard deviations:

$$\begin{aligned} WG^{r}_{x_2,y_2}IG^{o}_{x_1,y_1} &= \mathrm{rot}_{o}\left(N_{gtobr}\ \exp\left(-\frac{(x_1-x_2+r)^2}{2\,(btogo_{sds}(2r))^2}-\frac{(y_1-y_2)^2}{2\,(btog_{sdl}(2r))^2}\right)\right)\\ o &\in \{0,\pi/4,\pi/2,3\pi/4,\pi,5\pi/4,3\pi/2,7\pi/4\ \} \end{aligned} \tag{S23}$$

The connections from inhibitory IG cells to object grouping cells follow a similar connection pattern as the B to G cell excitation, except with the antipreferred orientation inhibiting the G cells:

$$\begin{aligned} WIG^{o+\pi}_{x_1,y_1}G^{r}_{x_2,y_2} &= \mathrm{rot}_{o+\pi}\left(N_{igtogr}\ \exp\left(-\frac{(x_1-x_2+r)^2}{2\,(btogo_{sds}r)^2}-\frac{(y_1-y_2)^2}{2\,(btog_{sdl}r)^2}\right)\right)\\ o &\in \{0,\pi/4,\pi/2,3\pi/4,\pi,5\pi/4,3\pi/2,7\pi/4\ \} \end{aligned} \tag{S24}$$

with the normalization coefficient N_{igtogr} obtained from:

$$igtog_w = \sum_{i=-2r}^{2r} WIG^{\pi}_{x-r,y+i}G^{r}_{x,y} \tag{S25}$$

as well as inhibition from orthogonal orientations:

$$\begin{aligned} W_oIG^{o\pm\pi/2}_{x_1,y_1}G^{r}_{x_2,y_2} &= \mathrm{rot}_{o\pm\pi/2}\left(N_{igtogro}\ \exp\left(-\frac{(x_1-x_2+r)^2}{2\,(btogo_{sds}r)^2}-\frac{(y_1-y_2)^2}{2\,(btog_{sdl}r)^2}\right)\right)\\ o &\in \{0,\pi/4,\pi/2,3\pi/4,\pi,5\pi/4,3\pi/2,7\pi/4\ \} \end{aligned} \tag{S26}$$

with the normalization coefficient $N_{igtogro}$ obtained from:

$$igtog_{wo} = \sum_{i=-2r}^{2r} W_oIG^{\pi/2}_{x-r,y+i}G^{r}_{x,y} \tag{S27}$$

It is assumed that the strength of the inhibition from the nonpreferred side of figure $igtog_w$ is equal to that of orthogonal preferred sides of figures $igtog_{wo}$, and each of them is equal to the value of the excitatory strength $btog_w$. Similar to the lateral connections in V2, this feedback loop has stronger but fewer and more specific excitatory connections, resulting in robust activity for specific inputs and more total inhibitory connection weights, resulting in little activity cased by nonspecific inputs.

Similarly, the connections from border-ownership cells with opposite side of figure preferences to contour grouping cells with the same preferred orientation consist of rotated 2D Gaussians, where $btogc_{sds}$ and $btog_{sdl}$ are the spreads of the Gaussian in the radial and tangential directions, respectively:

$$\begin{aligned} WB^{o_1}_{x_1,y_1}G^{o_2}_{x_2,y_2} &= \mathrm{rot}_{o_1}\left(N_{btogr}\ \exp\left(-\frac{(x_1-x_2)^2}{2\,(btogc_{sds}r)^2}-\frac{(y_1-y_2)^2}{2\,(btog_{sdl}r)^2}\right)\right) \\ &\sin^2(o_1-o_2)=1 \\ &o_1\in\{0,\pi/4,\pi/2,3\pi/4,\pi,5\pi/4,3\pi/2,7\pi/4\ \} \\ &o_2\in\{0,\pi/4,\pi/2,3\pi/4\} \end{aligned} \tag{S28}$$

where the normalization coefficient N_{btogr} is chosen such that

$$btog_w=\sum_{i=-2r}^{2r} WB^0_{x,y+i}G^0_{x,y} \tag{S29}$$

There is also excitation from other orientations, in order to explain the orientation dependence of V4 neurons:

$$\begin{aligned} W_oB^{o_1}_{x_1,y_1}G^{o_2}_{x_2,y_2} &= \frac{3}{4}\,\mathrm{rot}_{o_1}\left(N_{btogo}\ \exp\left(-\frac{(x_1-x_2)^2}{2\,(btogc_{sds}r)^2}-\frac{(y_1-y_2)^2}{2\,(btog_{sdl}r)^2}\right)\right) \\ &\sin^2(o_1-o_2)=\frac{\sqrt{2}}{2} \\ W_oB^{o_1}_{x_1,y_1}G^{o_2}_{x_2,y_2} &= \frac{1}{4}\,\mathrm{rot}_{o_1}\left(N_{btogo}\ \exp\left(-\frac{(x_1-x_2)^2}{2\,(btogc_{sds}r)^2}-\frac{(y_1-y_2)^2}{2\,(btog_{sdl}r)^2}\right)\right) \\ &\sin^2(o_1-o_2)=0 \\ &o_1\in\{0,\pi/4,\pi/2,3\pi/4,\pi,5\pi/4,3\pi/2,7\pi/4\ \} \\ &o_2\in\{0,\pi/4,\pi/2,3\pi/4\} \end{aligned} \tag{S30}$$

with the normalization coefficient N_{btogo} obtained from:

$$btog_{wo}=\sum_{i=-2r}^{2r} WB^0_{x,y+i}G^0_{x,y} \tag{S31}$$

The strength of the border-ownership to grouping connections $btog_w$, is a scaling parameter and was chosen to be 0.125, since in the model there are 4 preferred orientations and two side-of-figure preferences (8 total orientations) for the border-ownership cells, each of which sends input to each grouping cell. Each orientation of border-ownership cells provides a 2D Gaussian input to the grouping cells, with the standard deviation on the direction orthogonal to the radius being 0.5 times the radius, while the standard deviation on the direction parallel to the radius is 0.1 times the radius. This standard deviation parallel to the radius is smaller than that for object grouping neurons (0.25 times the radius) to account for higher selectivity to contours.

The feedback from the grouping cells also follows the spatial pattern of the B to grouping connections. The feedback to E and B are similar, although E cells receive feedback with twice the standard deviations to account for the higher number of neurons in the V1 layer:

$$\begin{aligned} WG^{o_1}_{x_2,y_2}B^{o_2}_{x_1,y_1} &= \mathrm{rot}_{o_2}\left(N_{gtobr}\ \exp\left(-\frac{(x_1-x_2)^2}{2\,(btogc_{sds}r)^2}-\frac{(y_1-y_2)^2}{2\,(btog_{sdl}r)^2}\right)\right) \\ &\sin^2(o_1-o_2)=1 \\ WG^{o_1}_{x_2,y_2}E^{o_1}_{x_1,y_1} &= \mathrm{rot}_{o_1}\left(N_{gtobr}\ \exp\left(-\frac{(x_1-x_2)^2}{2\,(btogc_{sds}(2r))^2}-\frac{(y_1-y_2)^2}{2\,(btog_{sdl}(2r))^2}\right)\right) \\ &o_1\in\{0,\pi/4,\pi/2,3\pi/4\} \\ &o_2\in\{0,\pi/4,\pi/2,3\pi/4,\pi,5\pi/4,3\pi/2,7\pi/4\ \} \end{aligned} \tag{S32}$$

Since the number of the grouping cells on a line is inverse proportional to their scale, the line integral of the weight is considered proportional to the radius of the G cell:

$$gtob_w=\sum_{i=-2r}^{2r} WG^o_{x,y}B^\pi_{x,y+i} \tag{S33}$$

The connection strength to the IE cells residing in V2 is assumed to be the same as the connection strength to the B cells. The value of $gtob_w=2/3$ is used for the model, similar to that for the object grouping cell to B cell feedback connections. As for the border ownership results, the weight of the feedback to edge cells is four times that to the border ownership cells $gtob_w=8/3$.

To fit the observed reaction time cost observed when irelevant objects are outside the focus of attention, a feedback from contour G to IG cells is introduced. This has the same pattern, but half the scaled weight as the feedback to B cells and twice its standard deviations:

$$\begin{aligned} WG^{o_1}_{x_2,y_2} IG^{o_2}_{x_1,y_1} &= \mathrm{rot}_{o_2}\left(N_{gtobr}\ \exp\left(-\frac{(x_1-x_2)^2}{2\,(btogo_{sds}(2r))^2}-\frac{(y_1-y_2)^2}{2\,(btog_{sdl}(2r))^2}\right)\right) \\ &\sin^2(o_1-o_2)=1 \\ &o_1 \in \{0,\pi/4,\pi/2,3\pi/4\} \\ &o_2 \in \{0,\pi/4,\pi/2,3\pi/4,\pi,5\pi/4,3\pi/2,7\pi/4\ \} \end{aligned} \tag{S34}$$

The connections from IG to contour grouping are nonspecific and similar to the connections from IG to object grouping cells, except without inhibition from other orientations:

$$\begin{aligned} WIG^{o_1}_{x_1,y_1} G^{o_2}_{x_2,y_2} &= \mathrm{rot}_{o_1}\left(N_{igtogr}\ \exp\left(-\frac{(x_1-x_2+r)^2}{2\,(btogo_{sds}r)^2}-\frac{(y_1-y_2)^2}{2\,(btog_{sdl}r)^2}\right)\right) \\ &o_1 \in \{0,\pi/4,\pi/2,3\pi/4,\pi,5\pi/4,3\pi/2,7\pi/4\ \} \\ &o_2 \in \{0,\pi/4,\pi/2,3\pi/4\} \end{aligned} \tag{S35}$$

with the normalization coefficient N_{igtogr} obtained from:

$$igtog_w = \sum_{i,j=-3}^{3} WIG^{o_1}_{x,y} G^{o_2}_{x+i,y+j} \tag{S36}$$

It is assumed that the strength of the inhibition $igtog_w$ is equal to the excitatory strength $btog_w$. Similar to the lateral connections in V2, this feedback loop has stronger but fewer and more specific excitatory connections, resulting in robust activity for specific inputs and more total inhibitory connection weights, resulting in little activity cased by nonspecific inputs.

Table 1 Parameter Values The scaling parameters with values that do not influence the behavior of the network are marked by *, see text.

Connection	Parameter	Value	Description
input	lE	1	input to edge cells
	$intoe_w$	1^*	input weight
attention	$Gatt_w$	0.07	maximal input
input	$Gatt_{sd}$	8	standard deviation
EtoIE	$etoie_w$	8	total strength
	$etoie_{sd}$	8	standard deviation
IEtoE	$ietoe_w$	-8	total strength
	$ietoe_{sd}$	8	standard deviation
EtoE	$etoe_w$	2/3	total strength
	$etoe_{sd}$	8	standard deviation
EtoB	$etob_w$	1^*	total strength
BtoIB	$btoib_w$	2	total strength
	$btoib_{sd}$	4	standard deviation
IBtoB	$ibtob_w$	-2	total strength
	$ibtob_{sd}$	4	standard deviation
BtoB	$btob_w$	2/3	total strength
	$btob_{wc}$	2/3	total strength
	$btob_{sd}$	4	standard deviation
BtoG	$btog_w$	0.125^*	line integral of weights
	$btog_{sdl}$	0.5	relative s.d. on tangential direction
	$btogo_{sds}$	0.25	relative s.d. on radial direction (object)
	$btogc_{sds}$	0.1	relative s.d. on radial direction (contour)
	r	16	radius (input pixels)
IGtoG	$igtog_w$	$-1/8$	line integral of weights
	$igtog_{wo}$	$-1/8$	line integral of weights
GtoB	$gtob_w$	2/3	line integral of weights
GtoIG	$gtoig_w$	1/3	line integral of weights
GtoE	$gtoe_w$	8/3	line integral of weights

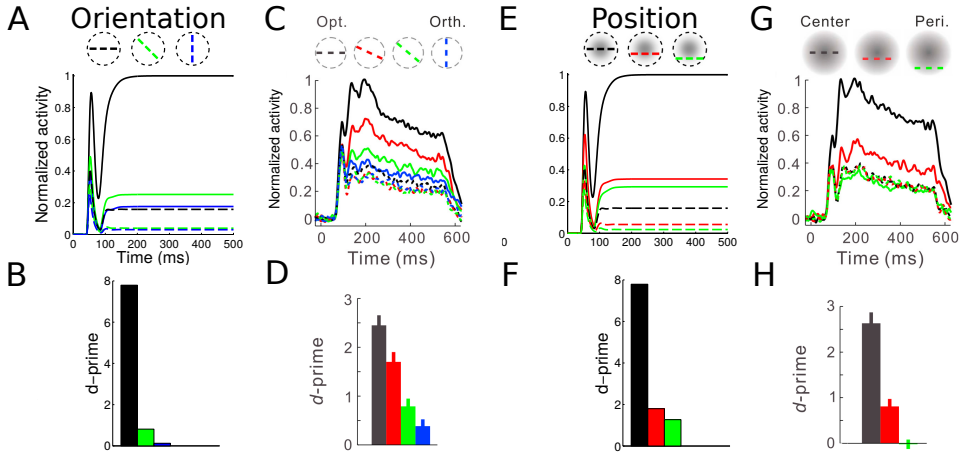

Fig. S1 Orientation and position dependence of contour integration in V4 G_c cells. The top row shows neuronal responses and the bottom row the contour-response d'. Line colors for each figure are indicated by the legends at the top of each column. Top row, solid lines indicate responses for the 7-bar contour pattern, while dashed lines indicate responses for the 1-bar (noise) pattern. Note that orientations were changed in variable steps based on the tuning curve of the neuron under study in the experimental data (panels C, D) while our simulation only allowed steps of $\pi/4$ (panels A,B). (A and B) Model results, orientation dependence. The neuronal responses (A) and the contour-response d' (B) decreased when the contour was rotated away from the preferred orientation. (C and D) Analogous experimental results, adapted from Chen et al (2014). (E and F) Model results, position dependence. The neuronal responses (E) and contour-response d' (F) decreased when the contour was translated away from the center of the V4 RF. (G and H) Analogous experimental results, adapted from Chen et al (2014). Panels C, D, G, and H are modified from Figure 3 of Chen et al (2014).

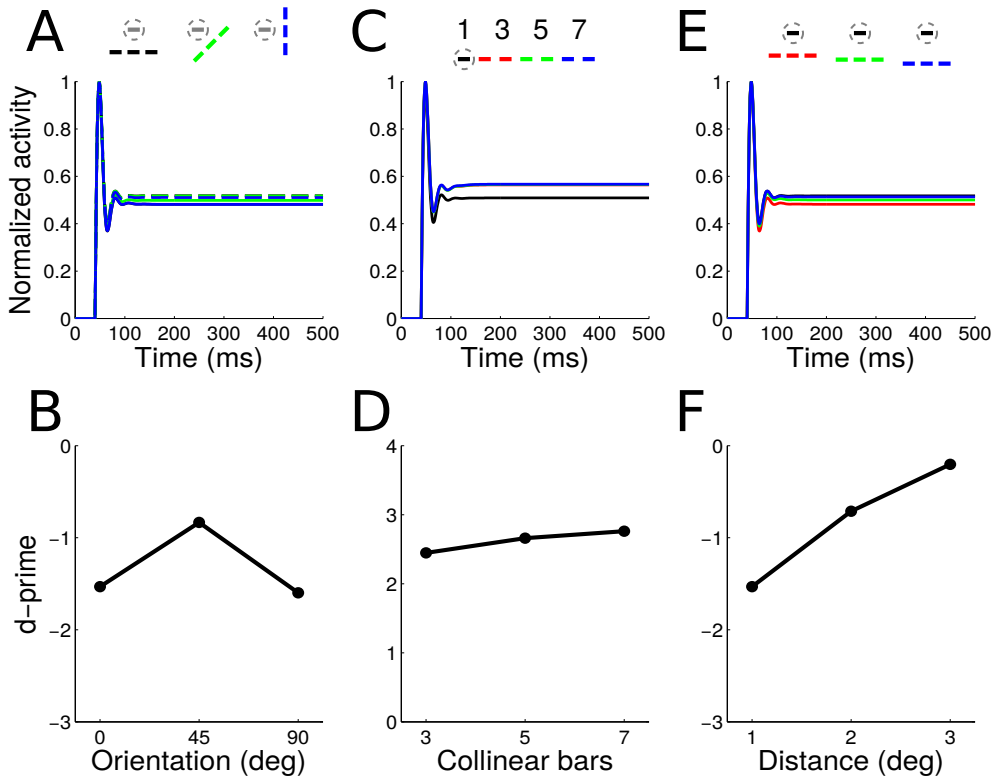

Fig. S2 Orientation and position dependence of contour integration in V1 E cells, model results. The top row shows neuronal responses and the bottom row the contour-response d'. Line colors for each figures are indicated by the legends at the top of each column. (A and B) Orientation dependence of background suppression. The neuronal responses (A) and the contour-response d' (B) increased for intermediate orientations of the background contour. In (A), solid and dashed lines correspond to the 7-bar contour and 1-bar noise patterns, respectively. (C and D) Contour integration on one end. The neuronal responses (C) and contour-response d' (D) increased when bars were added to only one side of the V1 RF. (E and F) Position dependence of background suppression. The neuronal responses (E) and contour-response d' (F) increased (approached zero) when the background contour was moved away from the center of the V1 RF.

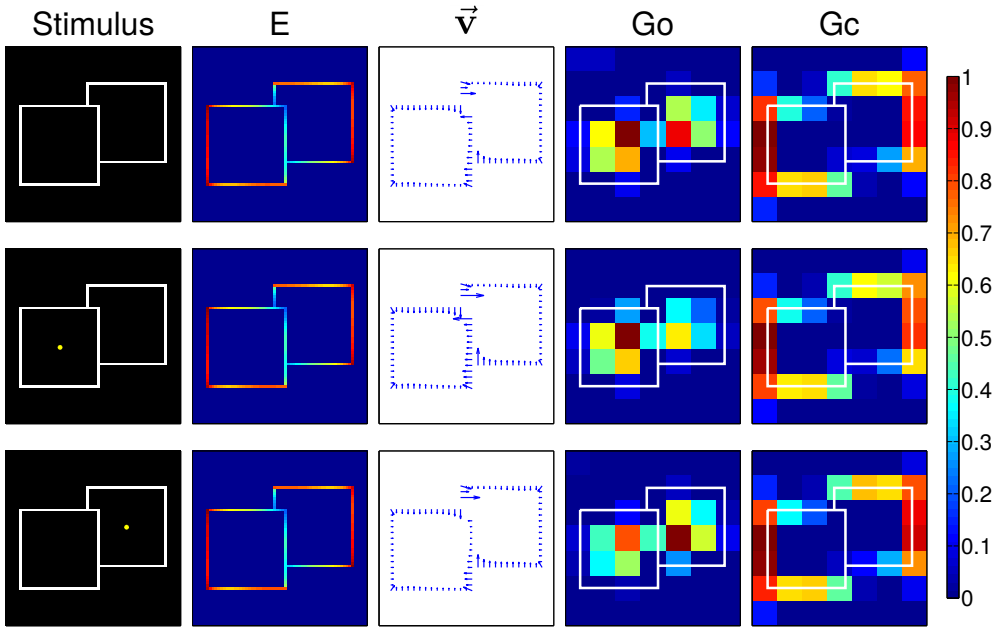

Fig. S3 Attention in the presence of multiple objects. Shown are (left to right) the input stimulus, the edge cell activity (E), the border ownership assignment along edges (shown as the vector modulation index $\vec{\mathbf{v}}$, section 2.5), the object grouping neuron activity (Go), and the contour grouping activity (Gc). The input stimulus is overlaid (white lines) on top of the grouping cell activities (columns 4 and 5) to aid visualizing the location of the two figures. Activities are normalized within each map, and warmer colors indicate higher activity (see color bar at right). The yellow dot indicates the locus of attention, which was applied at the level of grouping neurons. In the absence of attention (top row) or when attention is directed to the foreground square (middle row), the edge between the figures is correctly assigned to the foreground. If attention is directed toward the background square (bottom row), the border ownership signal of this edge is greatly reduced, consistent with experimental observations (Qiu et al, 2007).

Even in the absence of attention, figure-ground segregation can be observed in the border-ownership assignment along the edges of the two squares, as well as in the object and contour grouping cell activity (Figure S3, row 1). Figure S3 shows the responses of different populations of neurons in our model for the different attention conditions. This figure should be compared with Figure 3 in Mihalas et al (2011) which is a model related to ours but which does not contain G_c cells. The figure shows that the approximate locations of the foreground and background squares are represented by two peaks in the activity of object grouping neurons (fourth column). Selectively attending to one object enhances the activity of grouping neurons corresponding to the attended object while simultaneously suppressing the activity of grouping neurons representing the unattended object. Attentional modulation at the grouping neuron level is then propagated back to border-ownership selective neurons along object boundaries via the feedback grouping circuitry of our model. Of particular interest is the center edge separating the foreground and background squares. When attention is directed to the foreground square, assignment of border ownership along this edge is strengthened relative to the unattended case (Figure S3, row 2). However, if attention is directed toward the background square, border-ownership modulation of the edge between the two squares is greatly reduced (Figure S3, row 3). These results are in agreement with the physiological evidence (Qiu et al, 2007), and demonstrate that grouping mechanisms provide a means to attend to objects in clutter. Functionally, when attention is directed towards the occluded object, suppression of the border-ownership signal along the occluding edge is useful because this edge is "owned" by the occluder and should not be included in the representation of the attended object (Craft et al, 2007).